# 基于HPLC-Q-TOF-MS和网络药理学分析板蓝根防治流感及COVID-19的作用机制

王星琪[1], 常 金[1], 张 倩[1], 林丽娜[1], 邵 平[2], 李 清[1*]

(1. 沈阳药科大学药学院, 辽宁 沈阳 110016; 2. 本溪国家中成药工程技术研究中心有限公司, 辽宁 本溪 117004)

**摘要**: 将板蓝根化学成分与网络药理学研究结合, 探讨板蓝根防治流感及新型冠状病毒肺炎 (corona virus disease 2019, COVID-19) 的潜在分子作用机制。采用高效液相色谱−四极杆飞行时间质谱 (HPLC-Q-TOF-MS) 技术鉴定出板蓝根体外化学成分70个, 入血成分33个; 对其中41种潜在药效成分进行网络药理学分析。结果表明, 板蓝根可通过调控蛋白激酶B1 (protein kinase B1, AKT1)、血清白蛋白 (serum albumin, ALB)、甘油醛-3-磷酸脱氢酶 (glyceraldehyde-3-phosphate dehydrogenase, GAPDH)、血管内皮生长因子A (vascular endothelial growth factor A, VEGFA)、酪氨酸蛋白激酶SRC (tyrosine-protein kinase SRC, SRC)、表皮生长因子受体 (epidermal growth factor receptor, EGFR)、细胞间黏附分子-1 (intercellular adhesion molecule-1, ICAM1) 等关键靶点以及低氧诱导因子-1 (hypoxia inducible factor-1, HIF-1)、血管内皮细胞生长因子 (vascular endothelial growth factor, VEGF)、肿瘤坏死因子 (tumor necrosis factor, TNF)、甲型流感、Toll样受体 (Toll-like receptors, TLR)、磷脂酰肌醇-3-激酶-蛋白激酶B (phosphatidylinositol-3-kinase-protein kinase B, PI3K-AKT) 和COVID-19等潜在信号通路防治流感和COVID-19。本研究初步阐述了板蓝根防治流感及COVID-19通过炎症反应、免疫调节以及病毒防御等作用机制, 为后续临床研究提供依据。本文所有动物实验均获得沈阳药科大学伦理委员会批准 (SYPU-IACUC-S2020-12.23-201)。

**关键词**: 板蓝根; 高效液相色谱−四极杆飞行时间质谱; 网络药理学; 流感; 新型冠状病毒肺炎; 作用机制

**中图分类号**: R917 **文献标识码**: A **文章编号**: 0513-4870(2022)10-3173-13

# The mechanism of Isatidis Radix in the prevention of influenza and COVID-19 by HPLC-Q-TOF-MS combined with network pharmacology

WANG Xing-qi[1], CHANG Jin[1], ZHANG Qian[1], LIN Li-na[1], SHAO Ping[2], LI Qing[1*]

(*1. School of Pharmacy, Shenyang Pharmaceutical University, Shenyang 110016, China; 2. NERC for the Pharmaceutics of Traditional Chinese Medicines, Benxi 117004, China*)

**Abstract**: We identified molecular mechanisms by which Isatidis Radix might prevent or mitigate influenza and corona virus disease 2019 (COVID-19) based on chemical composition and network pharmacology. High performance liquid chromatography coupled to tandem quadrupole time-of-flight mass spectrometry (HPLC-Q-TOF-MS) was used to analyze the components of Isatidis Radix. Seventy compounds were identified, of which 33 prototype compounds entered the blood. Network pharmacological analysis of 41 potential active components demonstrated that Isatidis Radix can regulate protein kinase B1 (AKT1), serum albumin (ALB), glyceraldehyde-3-phosphate dehydrogenase (GAPDH), vascular endothelial growth factor A (VEGFA), tyrosine-protein kinase SRC (SRC), epidermal growth factor receptor (EGFR), intercellular adhesion molecule-1 (ICAM1) and other key genes, which have preventive effects on influenza and COVID-19 through hypoxia inducible factor-1 (HIF-1), vascular

收稿日期: 2022-04-16; 修回日期: 2022-08-10.

*通讯作者 Tel: 86-24-43510589, E-mail: lqyxm@hotmail.com

DOI: 10.16438/j.0513-4870.2022-0455

endothelial growth factor (VEGF), tumor necrosis factor (TNF), influenza A, Toll-like receptor (TLR), phosphatidylinositol-3-kinase-protein kinase B (PI3K-AKT), COVID-19 and other signaling pathways. This study identifies mechanisms by which Isatidis Radix might act against influenza and COVID-19 that are related to the inflammatory response, immunomodulation and viral defense, and provides a basis for subsequent clinical research. All animal experiments were approved by the Ethics Committee of Shenyang Pharmaceutical University (SYPU-IACUC-S2020-12.23-201).

**Key words**: Isatidis Radix; HPLC-Q-TOF-MS; network pharmacology; influenza; COVID-19; mechanism

流感一直是全球公共卫生面临的挑战, 具有传染性强, 潜伏期短, 发病率高等特点。近年出现的新型冠状病毒肺炎 (corona virus disease 2019, COVID-19) 更是严重危害人类生命健康的世界性传染病之一。两种疾病均属于病毒性传染病。目前预防和治疗手段主要是接种疫苗和使用抗病毒药物, 但随着病毒抗原的变异, 疫苗的保护作用会逐渐降低[1]。中医药在防治疫病中经验颇丰, 在流感和COVID-19的防治中起着重要作用[2-5]。

板蓝根源于《神农本草经》, 能够通过抗菌、抗病毒、抗炎和免疫调节作用达到清热解毒、凉血利咽的功效[6]。其化学成分主要包括生物碱类、木脂素类、核苷类、氨基酸类、有机酸类等[7]。板蓝根及其制剂在临床上常用于预防和治疗流行性感冒、肺炎、皮肤科疾病、肝胆疾病等病症[8,9], 并且板蓝根对于COVID-19的预防和治疗具有积极作用[10]。目前有关板蓝根单一成分抗病毒的药效研究较为深入[11-15], 部分研究仅借助在线数据库或体外成分对含有板蓝根的复方中药抗炎抗病毒作用进行网络药理学分析[16-23]。而基于中药“多成分−多靶点”的特点对板蓝根单味药抗病毒作用机制的研究较少, 有研究仅通过单一数据库筛选成分分析板蓝根抗新冠肺炎作用[24], 有必要综合体内外化学成分研究结合生物信息技术全面阐述板蓝根防治流感和COVID-19的作用机制。

网络药理学通过构建网络实现中药“活性成分−靶点−作用通路”的整体分析, 为中药作用机制的研究提供了新方法[25]。因此, 本文利用高效液相色谱−四极杆飞行时间质谱 (HPLC-Q-TOF-MS) 方法筛选出板蓝根入血成分以及有文献支持的有效成分, 与网络药理学结合, 预测板蓝根防治流感以及COVID-19的作用靶点和作用机制, 为临床诊疗及药物研究提供参考。

## 材料与方法

**仪器** Agilent 1260 Infinity 高效液相色谱 (美国安捷伦公司) 和 TripleTOF™ 5600$^+$四极杆−飞行时间质谱仪 (美国 AB Sciex 公司); Analyst® TF v1.6 软件、PeakView® v2.2.0 软件、MasterView™ v1.1 软件、LibraryView™ v1.0 软件 (美国 Sciex 公司); AB135-S 型电子分析天平 (瑞士 Mettler Toledo 公司); DZTW 调温电热套 (北京市永光明医疗仪器厂); RE-52A 型旋转蒸发仪和 SHZ-III 型循环水真空泵 (上海亚荣生化仪器厂); GENIUS 3 旋涡混合器 (德国 IKA 公司); TGL-16 型高速台式低温离心机 (湖南湘仪离心机仪器有限公司); MTN-2800D 型氮吹浓缩仪 (天津奥特赛恩斯仪器有限公司); KQ5200B 型超声波清洗器 (昆山市超声仪器有限公司)。

**试剂** (*R*,*S*)-告依春、尿苷、鸟苷、腺苷、胞苷、腺嘌呤、靛玉红、靛蓝、靛苷、吲哚-3-甲醛、水杨酸、吲哚-3-乙腈 (成都克洛玛生物科技有限公司, 批号: CHB180329、CHB180121、CHB180118、CHB210104、CHB201228、CHB201104、CHB180206、CHB180226、CHB210126、CHB201116、CHB201204、CHB210714, 纯度均为 HPLC ≥ 98%)。纯净水 (杭州娃哈哈有限公司); 甲醇 (色谱纯, 美国 Fisher 有限公司); 甲酸 (色谱纯, 天津市大茂化学试剂厂)。

**药材** 板蓝根饮片 (批号: 1811410111, 河北) 经沈阳药科大学中药学院王东教授鉴定为十字花科植物菘蓝 *Isatis indigotica* Fort. 的干燥根。

**实验动物** 雄性健康 Wistar 大鼠 12 只 [许可证号: SYXK (辽) 2020-0001], 体重 180～220 g, 由沈阳药科大学动物实验中心提供, 在沈阳药科大学 SPF 级动物实验室的独立送回风净化笼中, 22 ℃、50% RH 恒温恒湿条件下适应性饲养 7 天后进行实验。所有动物实验均获得沈阳药科大学伦理委员会批准 (SYPU-IACUC-S2020-12.23-201)。

### 板蓝根体外化学成分研究

色谱条件 ZORBAX Eclipse plus C18 色谱柱 (150 mm × 4.6 mm, 3.5 μm); 流动相: 0.1% 甲酸水 (A)−0.1% 甲酸甲醇 (B), 梯度洗脱程序为 0～3 min, 5% B; 3～15 min, 5%～30% B; 15～35 min, 30%～95% B; 35～40 min, 95% B; 40～40.1 min, 95%～5% B; 40.1～45 min, 5% B。流速: 1 mL·min$^{-1}$; 分流比 1∶1; 柱温: 30 ℃; 进样量: 5 μL; 自动进样器温度: 4 ℃。

质谱条件 采取电喷雾离子源 (ESI), 正、负离子模式均进行采集。离子喷雾电压正离子模式下为 5 500 V,

负离子模式下为−4 500 V, 源温度为550 ℃; 雾化气 ($N_2$) 压力为50 psi, 辅助气 ($N_2$) 压力为50 psi, 气帘气 ($N_2$) 压力为30 psi。TOF MS模式下扫描范围为 *m/z* 50～1 600 Da; 去簇电压 (DP) 为±80 V; 碰撞能为 ±10 V; TOF MS/MS模式下扫描范围为 *m/z* 50～1 600 Da; 去簇电压 (DP) 为±80 V; 碰撞能为±35 V。

对照品溶液的制备　分别取对照品 (*R*,*S*)-告依春、尿苷、鸟苷、腺苷、胞苷、腺嘌呤、靛玉红、靛蓝、靛苷、吲哚-3-甲醛、水杨酸和吲哚-3-乙腈适量, 精密称定, 用甲醇溶解配制成20 μg·mL$^{-1}$的混合对照品溶液。

供试品溶液的制备　称取板蓝根饮片适量置于圆底烧瓶中, 加入8倍量纯化水, 浸泡12 h, 加热回流提取2 h, 趁热过滤提取液; 向圆底烧瓶中加入6倍量纯化水, 回流提取1 h, 趁热过滤, 合并2次提取液, 加热浓缩至1.5 g·mL$^{-1}$的板蓝根水提液, 用于板蓝根入血成分的研究。精密量取两份, 加入适量水或甲醇稀释, 制成相当于每1 mL含生药0.375 g的药液, 经0.22 μm滤膜滤过, 于4 ℃冰箱保存。

**板蓝根入血成分研究**

血浆样品的采集　将大鼠随机分成两组灌胃给予板蓝根水提液, 给药剂量为5.04和10.08 g·kg$^{-1}$, 连续灌胃14天, 收集给药前与给药后0.5、1、2、4和6 h的血浆样品。血浆样品采用从大鼠眼眶静脉采集至肝素化的灭菌EP管内立即离心 (4 000 r·min$^{-1}$, 10 min) 方式, 将各时间点的血浆样品进行混合, 储存于−80 ℃冰箱中待用。

血浆样品的预处理　取1 mL血浆样品, 添加3 mL甲醇进行沉淀蛋白处理, 涡旋混匀 (3 min), 离心 (12 000 r·min$^{-1}$, 4 ℃, 5 min), 上清液转移至EP管中, 置于30 ℃氮气流下吹干。残渣添加50 μL甲醇进行复溶, 涡旋 (3 min), 超声 (5 min), 离心 (12 000 r·min$^{-1}$, 4 ℃, 5 min), 取上清液进行仪器分析。

色谱条件和质谱条件　与板蓝根体外化学成分研究色谱条件和质谱条件一致。

数据分析　参考CNKI、PubMed、Web of Science等数据库, 构建板蓝根化学成分数据库, 包含化学成分的名称、化学式、相对分子质量和特征碎片等。借助PeakView® V.2.2软件, 参考对照品以及数据库提供的保留时间、碎片信息对板蓝根中的成分进行定性分析与分类。

**网络药理学分析**

活性成分筛选　在体外成分鉴定结果的基础上, 符合以下条件之一的成分作为活性成分: ① 本实验中鉴定出的入血成分; ② 中国药典 (2020年版) 中规定的指标成分; ③ 有文献明确记载的活性成分。

活性成分与疾病的靶点筛选　选择Swiss Target Prediction数据库 (http: //www. swisstargetprediction.ch/) 置信度排名前30的靶点和PharmMapper数据库 (http://www.lilab-ecust.cn/pharmmapper/) 得分排名前30的靶点, 合并删除重复项, 得到活性成分靶点。在CTD数据库 (http://ctdbase.org/) 中, 选择Disease, 分别以关键词“influenza”和“COVID-19”进行搜索, 保留在gene项下Direct Evidence项中有“M” (疾病的生物标志物或在病因中起作用的靶点) 和“T” (疾病治疗靶点) 标记的靶点。在GeneCards数据库 (https://www.genecards.org/) 中, 分别以关键词“influenza”、“antiinfluenza”、“anti-influenza”和“COVID-19”进行搜索, 保留Inference Score≥0.8的靶点。分别合并两个数据库的所有靶点并删除重复项, 得到疾病相关靶点。将活性成分靶点与疾病靶点取交集, 得到板蓝根防治流感以及COVID-19的潜在靶点, 利用Cytoscape 3.8.1构建“成分−靶点”网络图, 将度值中位数值及以上的成分选作核心成分。

蛋白互作网络 (protein-protein interaction, PPI) 构建与分析　将“活性成分−疾病”潜在靶点输入STRING数据库 (https://string-db.org/), 物种选择“Homo sapiens”, 以tsv格式保存结果并在Cytoscape 3.8.1中打开, 利用cytoNCA插件计算靶点的点度中心性 (degree centrality, DC)、中介中心性 (betweenness centrality, BC)、接近中心性 (closeness centrality, CC), 以三者中位数及以上的交集靶点作为关键靶点。

关键靶点的功能和通路富集分析　将关键靶点输入DAVID数据库 (https://david.ncifcrf.gov/) 进行基因本体论 (gene ontology, GO) 和京都基因与基因组百科全书 (Kyoto encyclopedia of genes and genomes, KEGG) 富集分析, 以$P < 0.05$为筛选条件获得相关结果。

分子对接　将获得的前5个核心成分以及前5个关键靶点进行分子对接。从PDB数据库 (https://www.pdbus.org/) 中选择带有阳性药或小分子配体的蛋白, 利用Pymol软件删除溶剂和配体, 在AutoDock Tools软件中补充氢原子并加电荷; 在PubChem数据库中下载 (https://pubchem.ncbi.nlm.nih.gov/) 核心成分的3D结构, 对其补充氢原子并加电荷。设置活性口袋在蛋白中原配体所在位置, 利用AutoDock Tools软件进行50次分子对接, 得到核心成分与关键靶点的结合能, 借助Pymol分析结合作用。

## 结果

### 1　板蓝根化学成分的HPLC-Q-TOF-MS分析

运用所建立的液相色谱串联高分辨质谱法进行分

析, 正、负离子基峰离子图 (BPC) 如图1所示。初步鉴定了 70 个化合物 (表 1), 包括 24 个生物碱类化合物、10 个氨基酸类化合物、8 个核苷类化合物、7 个木脂素类化合物、7 个芳香酸及其衍生物、4 个脂类及脂肪酰基类化合物、2 个苯丙素类化合物、1 个黄酮类化合物和 7 个其他类化合物, 并鉴定出 33 种入血原形成分, 所鉴定的化合物质量误差均小于 5 ppm。

## 2 板蓝根活性成分及疾病靶点的筛选

对 33 个入血成分和其他 8 个有文献[14,15,26-30]记载具有活性的成分 (次黄嘌呤、鸟苷、直铁线莲宁 B、异落叶松脂醇、异牡荆苷、色胺酮、靛玉红和靛蓝) 进行靶点筛选, 共得到靶点 572 个; 按上述方法筛选出流感相关靶点 1 171 个, COVID-19 相关靶点 1 724 个, 构建韦恩图 (图 2) 得到板蓝根防治流感的潜在靶点 94 个, 防治 COVID-19 的潜在靶点 86 个。构建“成分−靶点”网络图 (图 3), 成分的形状和度值呈正相关, 将度值在中位数及以上的成分作为核心成分, 得到板蓝根防治流感的 27 个核心成分和防治 COVID-19 的 25 个核心成分。

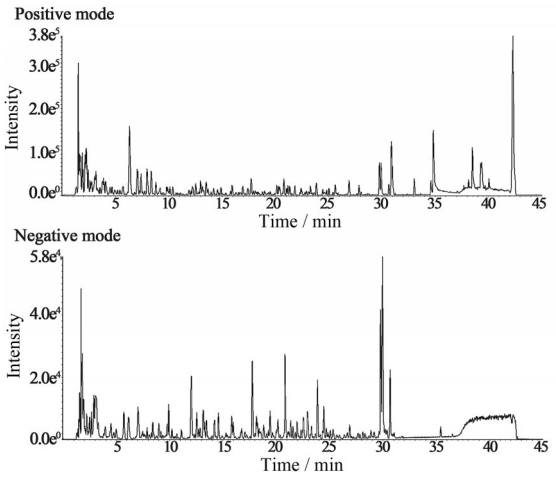


**Figure 1** Base peak chromatogram of Isatidis Radix in both positive and negative modes

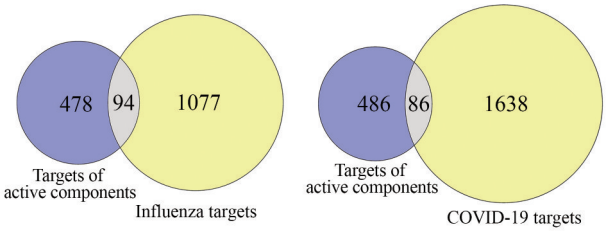


**Figure 2** Venn diagram of Isatidis Radix-Influenza targets and Isatidis Radix-COVID-19 targets

## 3 PPI 分析筛选核心靶点

按照上述方法得到 PPI 网络图 (图 4), 靶点的颜色、大小和度值呈正相关。取 DC、BC、CC 中位数及以上的交集靶点作为关键靶点, 得到板蓝根防治流感的 39 个关键靶点和防治 COVID-19 的 34 个关键靶点。

**Table 1** Identification analysis results of ingredients in Isatidis Radix. a: Confirmed by authentic standards; b: Considered the component of the sample diluted with methanol; c: Absorptive ingredients in rat plasma

| No. | Compound | Formula | Ion adduction | Measured mass (*m/z*) | Error /ppm | $t_R$ /min | Product ions (*m/z*) | *In vivo* |
|---|---|---|---|---|---|---|---|---|
| 1 | Histidine | $C_6H_9N_3O_2$ | $[M+H]^+$ | 156.076 6 | −1.0 | 1.45 | 83.060 0, 93.0437, 110.069 9 | |
| 2 | Arginine | $C_6H_{14}N_4O_2$ | $[M+H]^+$ | 175.118 8 | −0.9 | 1.50 | 60.057 3, 70.066 0, 130.097 5, 158.092 8 | c |
| 3 | Anthranilic acid | $C_7H_7NO_2$ | $[M+H]^+$ | 138.054 4 | −3.9 | 1.63 | 65.039 7, 78.034 4, 92.050 1, 138.055 2 | c |
| 4 | Proline | $C_5H_9NO_2$ | $[M+H]^+$ | 116.070 5 | −1.0 | 1.66 | 70.066 0 | c |
| 5 | Sucrose | $C_{12}H_{22}O_{11}$ | $[M−H]^-$ | 341.108 6 | −0.9 | 1.76 | 89.026 1, 119.036 4, 161.046 4, 179.056 8 | c |
| 6 | Valine | $C_5H_{11}NO_2$ | $[M+H]^+$ | 118.086 1 | −1.0 | 2.09 | 55.056 5, 56.051 7, 57.059 3, 72.082 0 | c |
| 7 | Cytidine[a] | $C_9H_{13}N_3O_5$ | $[M+H]^+$ | 244.092 6 | −1.0 | 2.18 | 95.024 4, 112.050 3 | c |
| 8 | Adenine[a] | $C_5H_5N_5$ | $[M+H]^+$ | 136.061 1 | −5.0 | 2.32 | 65.014 4, 92.023 9, 119.033 6, 136.059 6 | c |
| 9 | Methionine | $C_5H_{11}NO_2S$ | $[M+H]^+$ | 150.057 9 | −3.0 | 2.52 | 56.051 3, 104.053 2, 133.031 7 | c |
| 10 | Nicotinic acid | $C_6H_5NO_2$ | $[M+H]^+$ | 124.038 9 | −3.7 | 2.68 | 53.040 9, 78.034 4, 79.042 7, 80.050 1, 124.039 4 | c |
| 11 | Allopurinol | $C_5H_4N_4O$ | $[M+H]^+$ | 137.045 2 | −4.3 | 3.31 | 110.033 5, 119.033 8, 120.018 5, 137.043 3 | |
| 12 | Isoleucine | $C_6H_{13}NO_2$ | $[M+H]^+$ | 132.101 6 | −2.6 | 3.76 | 69.069 8, 86.095 1 | |
| 13 | Tyrosine | $C_9H_{11}NO_3$ | $[M+H]^+$ | 182.080 5 | −3.6 | 3.92 | 91.054 3, 119.049 0, 136.075 3, 147.043 5, 165.054 6 | c |
| 14 | Uridine[a] | $C_9H_{12}N_2O_6$ | $[M+H]^+$ | 245.076 5 | −1.4 | 3.94 | 70.029 7, 96.007 6, 113.034 3 | c |

Continued

| No. | Compound | Formula | Ion adduction | Measured mass (*m/z*) | Error /ppm | $t_R$ /min | Product ions (*m/z*) | *In vivo* |
|---|---|---|---|---|---|---|---|---|
| 15 | Uracil | $C_4H_4N_2O_2$ | $[M+H]^+$ | 113.034 2 | −2.9 | 3.94 | 53.003 2, 70.028 3, 96.006 6, 113.030 9 | c |
| 16 | Leucine | $C_6H_{13}NO_2$ | $[M+H]^+$ | 132.101 4 | −3.9 | 4.08 | 86.097 0 | |
| 17 | Adenosine[a] | $C_{10}H_{13}N_5O_4$ | $[M+H]^+$ | 268.104 3 | 0.9 | 6.32 | 136.061 0 | c |
| 18 | Hypoxanthine | $C_5H_4N_4O$ | $[M+H]^+$ | 137.045 3 | −3.3 | 6.91 | 110.035 6, 119.035 2, 120.021 6, 137.046 4 | |
| 19 | Guanosine[a] | $C_{10}H_{13}N_5O_5$ | $[M+H]^+$ | 284.099 2 | 0.9 | 7.06 | 110.035 3, 135.029 9, 152.056 2 | |
| 20 | Guanine | $C_5H_5N_5O$ | $[M+H]^+$ | 152.056 5 | −1.2 | 7.06 | 110.034 2, 135.029 1, 152.054 9 | |
| 21 | Matrine | $C_{15}H_{24}N_2O$ | $[M+H]^+$ | 249.196 2 | 0.1 | 7.75 | 148.111 0 | c |
| 22 | Phenylalanine | $C_9H_{11}NO_2$ | $[M+H]^+$ | 166.085 9 | −2.4 | 7.97 | 77.039 4, 103.054 2, 120.080 3 | |
| 23 | Hexose-phenylalanine | $C_{15}H_{21}NO_7$ | $[M-H]^-$ | 326.123 4 | −3.3 | 8.94 | 164.070 8, 236.091 3 | |
| 24 | 4-Pentenamide | $C_5H_9NO$ | $[M+H]^+$ | 100.075 8 | 0.8 | 9.05 | 57.071 7, 83.052 0, 100.076 0 | c |
| 25 | (*R*,*S*)-Goitrin[a] | $C_5H_7NOS$ | $[M+H]^+$ | 130.032 0 | −3.8 | 9.11 | 60.975 9, 70.066 3, 77.039 6, 78.033 7, 103.054 4 | c |
| 26 | Dihydroxybenzoic acid glucoside | $C_{13}H_{16}O_9$ | $[M-H]^-$ | 315.071 4 | −2.3 | 12.03 | 109.030 5, 153.019 2 | |
| 27 | Tryptophan | $C_{11}H_{12}N_2O_2$ | $[M+H]^+$ | 205.096 7 | −2.3 | 12.23 | 118.065 2, 146.060 0, 188.070 6 | |
| 28 | Indole-3-acetonitrile-6-*O*-*β*-*D*-glucopyranoside | $C_{16}H_{18}N_2O_6$ | $[M+HCOO]^-$ | 379.114 0 | 1.2 | 13.15 | 144.045 6, 171.055 9, 306.096 2, 333.106 6 | c |
| 29 | Indican[a] | $C_{14}H_{17}NO_6$ | $[M+H]^+$ | 296.112 7 | −0.5 | 13.25 | 106.065 9, 134.060 2, 149.022 7, 164.092 9 | c |
| 30 | Oxindole | $C_8H_7NO$ | $[M+H]^+$ | 134.059 5 | −3.7 | 13.25 | 77.139 1, 89.039 0, 91.051 2, 106.063 6, 116.048 4, 134.057 4 | c |
| 31 | *cis*-Coniferin | $C_{16}H_{22}O_8$ | $[M+Na]^+$ | 365.120 4 | −0.8 | 14.57 | 185.041 1, 202.058 4, 237.096 3 | c |
| 32 | 2,3-Dihydro-1*H*-pyrrolo[2,1-*c*][1,4]benzodiazepine-5,11(10*H*,11a*H*)-dione | $C_{12}H_{12}N_2O_2$ | $[M+H]^+$ | 217.097 0 | −0.7 | 14.59 | 74.024 7, 144.080 7 | c |
| 33 | Isaindigodione | $C_{18}H_{18}N_2O_4$ | $[M+H]^+$ | 327.133 9 | −0.3 | 14.89 | 145.076 4, 173.071 0, 201.102 4 | c |
| 34 | Benzoic acid | $C_7H_6O_2$ | $[M-H]^-$ | 121.029 8 | 2.7 | 15.79 | 92.028 2, 121.030 2 | |
| 35 | Syringin | $C_{17}H_{24}O_{19}$ | $[M+NH_4]^+$ | 390.175 7 | −0.4 | 15.95 | 105.070 2, 133.064 1, 161.059 6, 193.086 0, 211.096 5 | |
| 36 | (*E*)-2-(2-Oxoindolin-3-ylidene) acetonitrile | $C_{10}H_6N_2O$ | $[M+H]^+$ | 171.054 8 | −2.7 | 16.84 | 77.033 9, 116.049 4 | c |
| 37 | 3-Indole acetamide | $C_{10}H_{10}N_2O$ | $[M+H]^+$ | 175.085 9 | −3.8 | 17.03 | 77.039 2, 103.053 8, 130.065 0 | c |
| 38 | Clemastanin B | $C_{32}H_{44}O_{16}$ | $[M+HCOO]^-$ | 729.261 4 | 1.8 | 17.76 | 329.137 5, 359.148 1, 521.199 5 | |
| 39 | 2-Hydroxy-1,4-benzenedicarboxylic acid | $C_8H_6O_5$ | $[M-H]^-$ | 181.014 2 | −0.4 | 19.64 | 93.036 2 | c |
| 40 | Lariciresinol-4-*O*-*β*-*D*-glucopyranoside | $C_{26}H_{34}O_{11}$ | $[M+HCOO]^-$ | 567.206 8 | −0.7 | 20.16 | 329.137 2, 359.470 0, 521.200 0 | |
| 41 | 1-Methoxyindole-3-acetamide | $C_{11}H_{12}N_2O_2$ | $[M+H]^+$ | 205.096 9 | −3.7 | 20.23 | 130.065 2, 160.075 1, 188.071 6 | c |
| 42 | Deoxyvasicinone | $C_{11}H_{10}N_2O$ | $[M+H]^+$ | 187.086 2 | −2.2 | 20.33 | 77.038 9, 115.053 2, 146.059 4 | c |
| 43 | Lariciresinol-4'-*O*-*β*-*D*-glucopyranoside | $C_{26}H_{34}O_{11}$ | $[M+HCOO]^-$ | 567.206 7 | −1.0 | 20.83 | 329.137 0, 359.148 2, 521.199 8 | |
| 44 | Matairesinol-4-*O*-*D*-glucopyranoside | $C_{26}H_{32}O_{11}$ | $[M+NH_4]^+$ | 538.227 7 | −1.0 | 20.85 | 137.059 4, 311.129 4, 359.152 8, 503.190 3 | |
| 45 | Ferulic acid | $C_{10}H_{10}O_4$ | $[M+H]^+$ | 195.052 2 | 0.2 | 20.93 | 89.038 9, 117.033 4, 145.028 0, 177.055 6 | |
| 46 | Indole-3-carbaldehyde[a] | $C_9H_7NO$ | $[M+H]^+$ | 146.059 7 | −2.1 | 21.07 | 54.039 7, 91.054 2, 117.057 2, 118.065 9 | c |
| 47 | 4-Hydroxyindole-3-carbaldehyde | $C_9H_7NO_2$ | $[M+H]^+$ | 162.054 2 | −4.9 | 21.14 | 89.040 4, 116.049 3, 144.048 2 | c |
| 48 | Conicaoside | $C_{27}H_{36}O_{12}$ | $[M+Na]^+$ | 575.209 4 | −0.8 | 21.33 | 413.157 8 | |
| 49 | Isolariciresinol | $C_{20}H_{24}O_6$ | $[M+HCOO]^-$ | 405.154 3 | −0.3 | 21.37 | 313.105 9, 344.125 2, 359.146 9 | |
| 50 | Pinoresinol glycoside | $C_{26}H_{32}O_{11}$ | $[M-H]^-$ | 519.186 0 | −2.3 | 21.77 | 151.038 1, 357.132 5, 519.184 5 | |
| 51 | Isovitexin | $C_{21}H_{20}O_{10}$ | $[M+H]^+$ | 433.112 6 | −0.7 | 22.47 | 313.069 9, 337.069 7, 349.071 4, 379.081 6, 397.092 1, 415.105 7 | |
| 52 | 3-(2′-Carboxyphenyl)-4(3*H*)-quinazolinone | $C_{15}H_{10}N_2O_3$ | $[M+H]^+$ | 267.076 4 | 0 | 22.64 | 120.044 0, 146.023 2, 239.080 9, 249.066 7 | c |
| 53 | Salicylic acid[a] | $C_7H_6O_3$ | $[M+H]^+$ | 139.038 7 | −2.1 | 22.87 | 65.042 1, 79.021 8, 93.037 3, 121.028 8, 130.066 7 | c |

Continued

| No. | Compound | Formula | Ion adduction | Measured mass (*m/z*) | Error /ppm | $t_R$ /min | Product ions (*m/z*) | *In vivo* |
|---|---|---|---|---|---|---|---|---|
| 54 | Indole-3-acetonitrile-2-*S*-*β*-*D*-glucopyranoside | $C_{16}H_{18}N_2O_5S$ | $[M+H]^+$ | 349.085 1 | −3.7 | 22.92 | 160.022 0, 187.032 6 | c |
| 55 | 3-Indoleacetonitrile[a] | $C_{10}H_8N_2$ | $[M+H]^+$ | 157.075 7 | −1.8 | 23.15 | 77.039 7, 103.054 9, 117.057 5, 130.065 3 | |
| 56 | 3-(2′-Hydroxyphenyl)-4(3*H*)-quinazolinone | $C_{14}H_{10}N_2O_2$ | $[M+H]^+$ | 239.081 3 | −0.7 | 24.20 | 120.044 1, 132.044 7, 211.088 7 | |
| 57 | Indole-3-acetonitrile-4-methoxy-2-*S*-*β*-*D*-glucopyranoside | $C_{17}H_{20}N_2O_6S$ | $[M+H]^+$ | 398.137 0 | −2.7 | 24.46 | 171.054 8, 179.039 8, 186.078 6, 219.059 0 | |
| 58 | *N*-Methoxy-indole-3-acetonitrile-2-*S*-*β*-*D*-glucopyranoside | $C_{17}H_{20}N_2O_6S$ | $[M+H]^+$ | 398.137 5 | −1.4 | 24.68 | 128.049 2, 161.029 1, 188.039 9, 187.032 2, 219.058 6 | |
| 59 | 1-Methoxyindole-3-carboxaldehyde | $C_{10}H_9NO_2$ | $[M+H]^+$ | 176.070 2 | −2.1 | 25.63 | 89.039 7, 104.050 3, 117.057 7, 133.052 4, 144.044 5, 161.047 0 | c |
| 60 | Tryptanthrin | $C_{15}H_8N_2O_2$ | $[M+H]^+$ | 249.065 5 | −1.5 | 28.80 | 130.029 2, 221.070 9 | |
| 61 | 9(*S*),12(*S*),13(*R*)-Trihydroxy-10(*E*),15(*Z*)-octadecadienoic acid | $C_{18}H_{32}O_5$ | $[M-H]^-$ | 327.216 1 | −5.0 | 29.79 | 171.102 5, 211.133 5, 221.116 8, 291.195 4 | |
| 62 | Panaquinquecol 1 | $C_{18}H_{28}O_3$ | $[M+H]^+$ | 293.210 8 | −1.0 | 29.93 | 91.054 4, 105.069 9, 107.086 6, 133.101 2, 147.116 5, 275.201 5 | |
| 63 | 9(*S*),10(*S*),11(*R*)-Trihydroxy-12(*Z*),15(*Z*)-octadecadienoic acid | $C_{18}H_{32}O_5$ | $[M-H]^-$ | 327.216 1 | −4.9 | 29.95 | 183.137 7, 211.132 4, 229.142 7, 291.194 4 | |
| 64 | 9,12,13-Trihydroxy-10(*E*)-octadecadienoic acid | $C_{18}H_{34}O_5$ | $[M-H]^-$ | 329.232 0 | −4.1 | 30.68 | 211.132 5, 229.143 6, 311.220 6 | |
| 65 | Indirubin[a,b] | $C_{16}H_{10}N_2O_2$ | $[M+H]^+$ | 263.081 2 | −1.3 | 31.19 | 132.043 6, 190.066 6, 206.081 1, 219.090 1, 235.088 5, 245.163 4 | |
| 66 | UNPD49053 | $C_{24}H_{30}O_6$ | $[M+H]^+$ | 415.211 1 | −0.9 | 32.41 | 91.054 7, 119.084 1, 135.079 3 | |
| 67 | Indigo[a,b] | $C_{16}H_{10}N_2O_2$ | $[M+H]^+$ | 263.081 0 | −2.0 | 32.99 | 165.070 2, 190.064 7, 219.091 9, 235.088 4, 245.164 5 | |
| 68 | LysoPC(18:3(6Z,9Z,12Z)) | $C_{26}H_{48}NO_7P$ | $[M+H]^+$ | 518.322 1 | −3.9 | 37.67 | 104.106 8, 146.981 6, 313.274 1, 459.248 4 | |
| 69 | LysoPC(16:0) | $C_{24}H_{50}NO_7P$ | $[M+H]^+$ | 496.338 8 | −2.0 | 37.67 | 104.107 1, 184.073 6, 313.275 5, 360.322 1, 478.330 3 | |
| 70 | Bis(2-ethylhexyl) phthalate | $C_{24}H_{38}O_4$ | $[M+H]^+$ | 391.284 2 | −0.2 | 40.57 | 71.085 4, 121.028 6, 149.022 6 | |

## 4 GO和KEGG富集分析

将得到的核心靶点在DAVID数据库中进行GO和KEGG富集分析。以$P < 0.05$为筛选条件得到板蓝根防治流感的GO分析结果中生物过程 (BP)、细胞组分 (CC) 和分子功能 (MF) 相关条目分别为270、46和56个, 板蓝根防治COVID-19的相关条目分别为152、30和40个。每组选取前10个重要结果绘制条形图, 以−lg*P*值来衡量GO富集程度 (图5)。防治流感的靶点蛋白主要参与细胞因子介导的信号通路、血管内皮生长因子受体信号通路、凋亡过程的负调控等生物过程, 作用于细胞质、大分子复合物等细胞组分, 调节酶结合、蛋白质结合等功能; 防治COVID-19的靶点蛋白主要参与蛋白水解、凋亡过程的负调控、病毒进入宿主细胞等生物过程, 作用于细胞表面、细胞膜等细胞组分, 调节酶结合、病毒受体活性等分子功能。

以$P < 0.05$为筛选条件选取前35个重要通路绘制气泡图, 以富集到该通路的核心靶点个数和−lg*P*值来衡量KEGG富集程度 (图6)。得到板蓝根防治流感的KEGG通路138个, 主要包括低氧诱导因子-1 (hypoxia inducible factor-1, HIF-1)、血管内皮细胞生长因子 (vascular endothelial growth factor, VEGF)、肿瘤坏死因子 (tumor necrosis factor, TNF)、甲型流感、Toll样受体 (Toll-like receptors, TLR) 等信号通路。防治COVID-19的KEGG通路91个, 主要富集在人类巨细胞病毒感染、冠状病毒-COVID-19、HIF-1、磷脂酰肌醇-3-激酶-蛋白激酶B (phosphatidylinositol-3-kinase-protein kinase B, PI3K-AKT)、甲型流感、TLR、TNF等信号通路。

## 5 分子对接

板蓝根防治流感的度值前5的核心成分 (色胺酮、依靛蓝酮、吲哚-3-乙腈-6-*O*-*β*-*D*-吡喃葡萄糖苷、1-甲氧基-吲哚-3-乙酰胺、[2,3-二氢-1*H*-吡咯并[2,1-*c*][1,4]苯并二氮杂䓬-5,11(10*H*,11a*H*)-二酮]) 和度值前5的关键靶点 [调控蛋白激酶B1 (protein kinase B1, AKT1)、血清白蛋白 (serum albumin, ALB)、甘油醛-3-磷酸脱氢酶 (glyceraldehyde-3-phosphate dehydrogenase, GAPDH)、血管内皮生长因子A (vascular endothelial growth factor A, VEGFA)、酪氨酸蛋白激酶SRC (tyrosine-protein kinase SRC, SRC)] 分子对接结果如表2。板蓝根防治

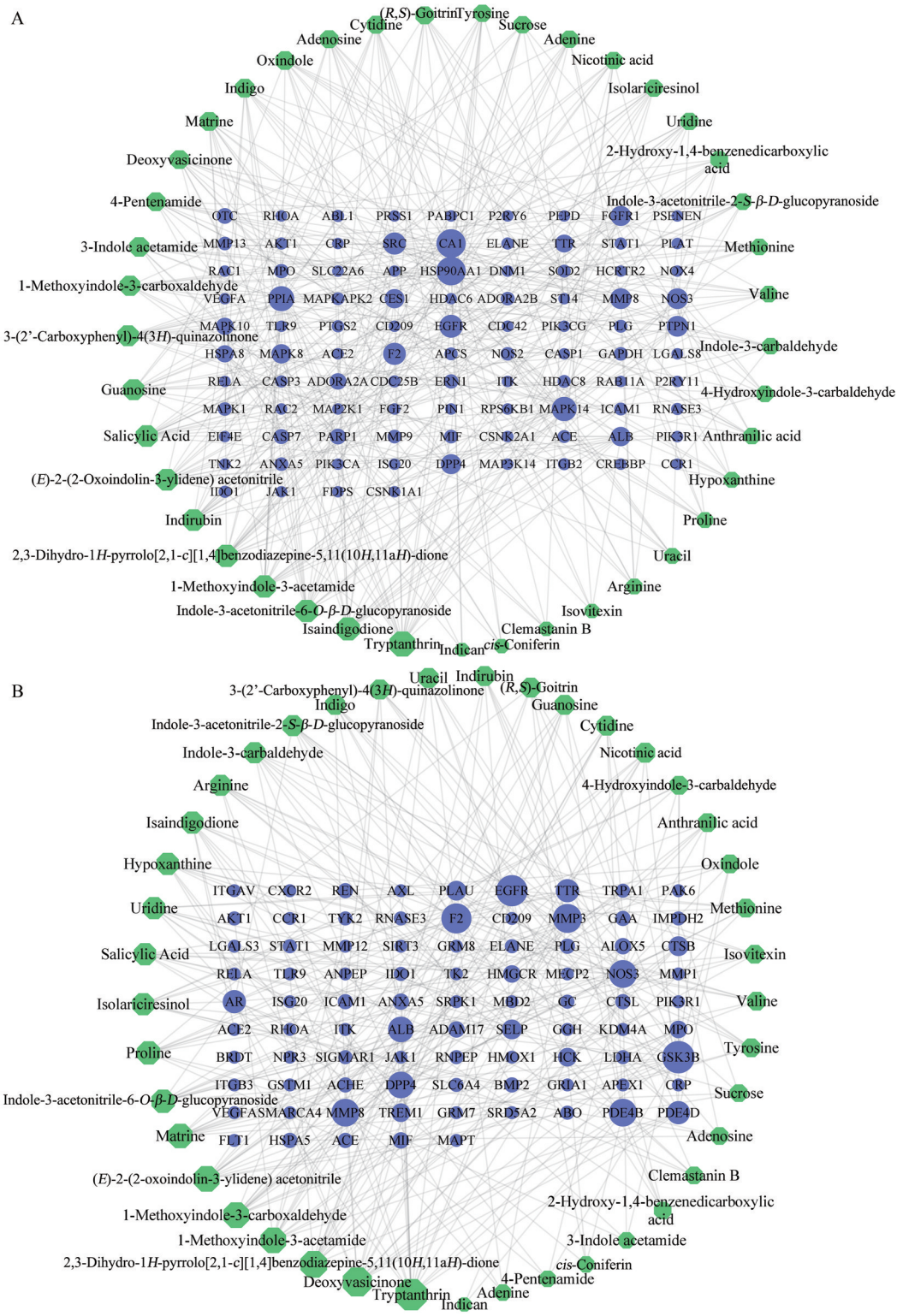


**Figure 3** The "component-target" network of Isatidis Radix-influenza (A) and Isatidis Radix-COVID-19 (B). Green hexagon: Active components; Purple circle: Disease-related targets

COVID-19的度值前五的核心成分 (色胺酮、脱氧鸭嘴花碱酮、[2,3-二氢-1*H*-吡咯并[2,1-*c*][1,4]苯并二氮杂䓬-5,11(10*H*,11a*H*)-二酮]、1-甲氧基吲哚-3-乙酰胺、1-甲氧基吲哚-3-甲醛) 和度值前5的关键靶点 [ALB、AKT1、VEGFA、表皮生长因子受体 (epidermal growth factor receptor, EGFR)、细胞间黏附分子-1 (intercellular adhesion molecule-1, ICAM1)] 分子对接结果如表3。

对接结果显示结合能全部小于−5 kcal·mol$^{-1}$, 表明

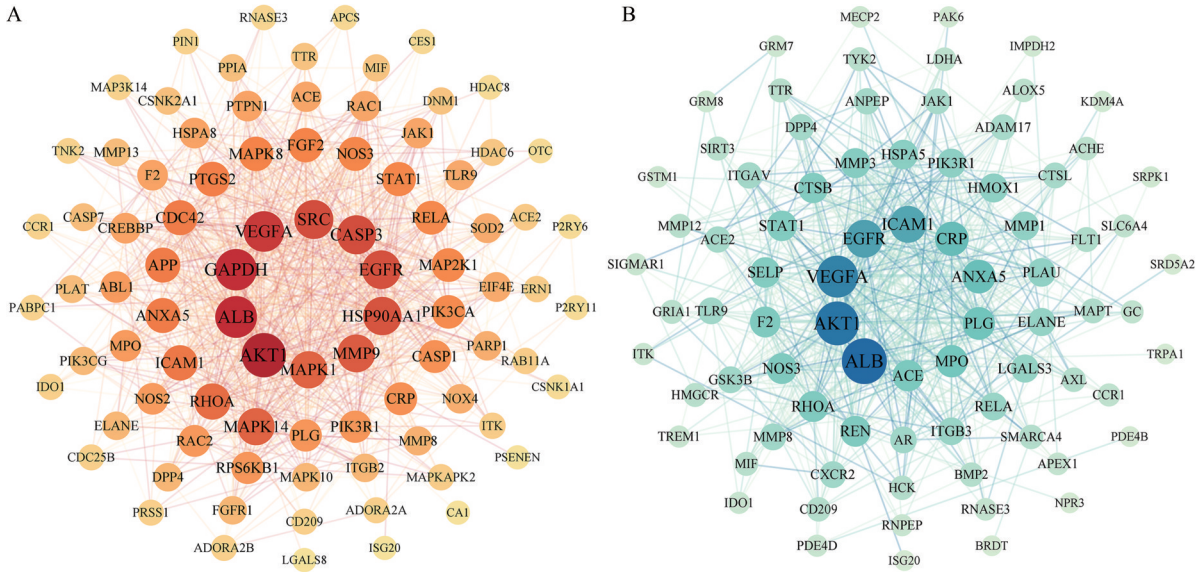


**Figure 4** Influenza-related (A) and COVID-19-related (B) PPI network regulated by Isatidis Radix based on analysis of string database. AKT1: Protein kinase B1; ALB: Serum albumin; GAPDH: Glyceraldehyde-3-phosphate dehydrogenase; VEGFA: Vascular endothelial growth factor A; SRC: Tyrosine-protein kinase SRC; EGFR: Epidermal growth factor receptor; ICAM1: Intercellular adhesion molecule-1

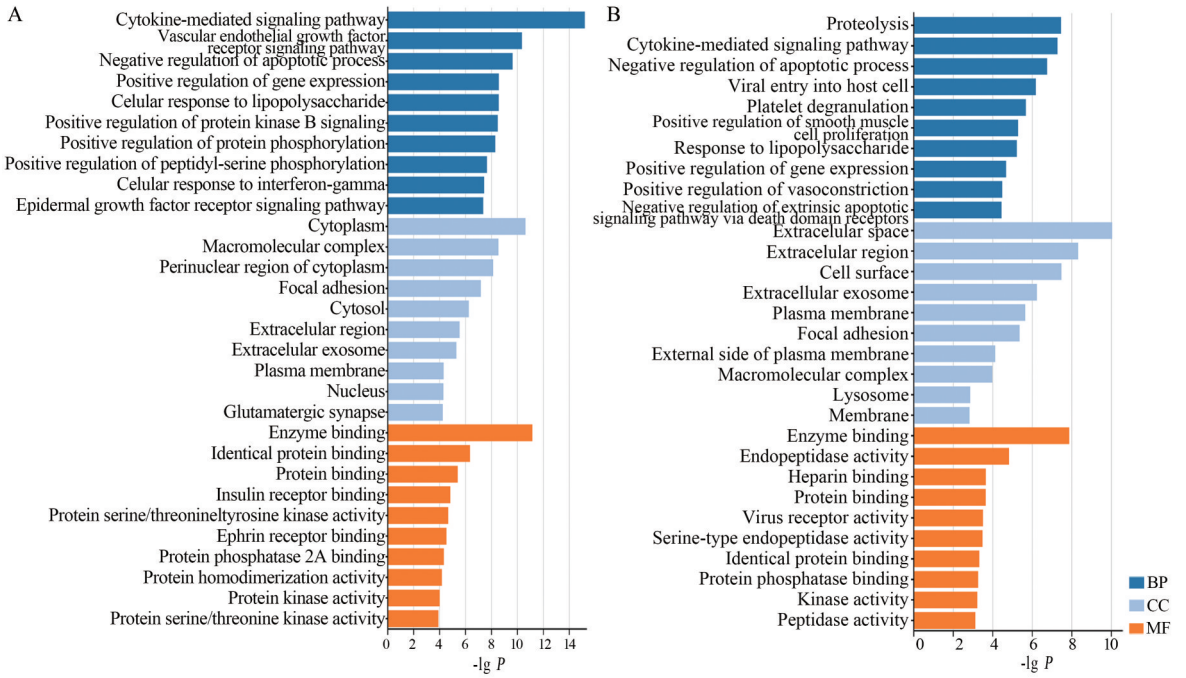


**Figure 5** GO enrichment analysis of influenza-related target proteins (A) and COVID-19-related target proteins (B). GO: Gene ontology; BP: Biological process; CC: Cellular component; MF: Molecular function

受体与配体之间结合良好; 且配体与受体的结合位点和阳性药 (受体原有的小配体) 与受体的结合位点一致, 说明药物和阳性药有相同的药效团, 能更有效地发挥作用。

## 讨论

流行性感冒是一种由流感病毒引起的呼吸道传染性疾病, 秋冬季节高发, 临床上患者常出现咳嗽、头痛、肌肉酸痛等不适[31]。COVID-19 是一种由新型冠状病毒引起的严重呼吸道传染性疾病, 潜伏期较长, 具有高死亡率[32]。板蓝根作为清热解毒的代表性中药之一, 对肺胃热盛所致疾病有很大疗效, 临床上用于治疗流感、肺炎、热毒发斑、咽肿疼腮、瘟疫等病症[7]。本研究结合 HPLC-Q-TOF-MS 技术和网络药理学策略, 从

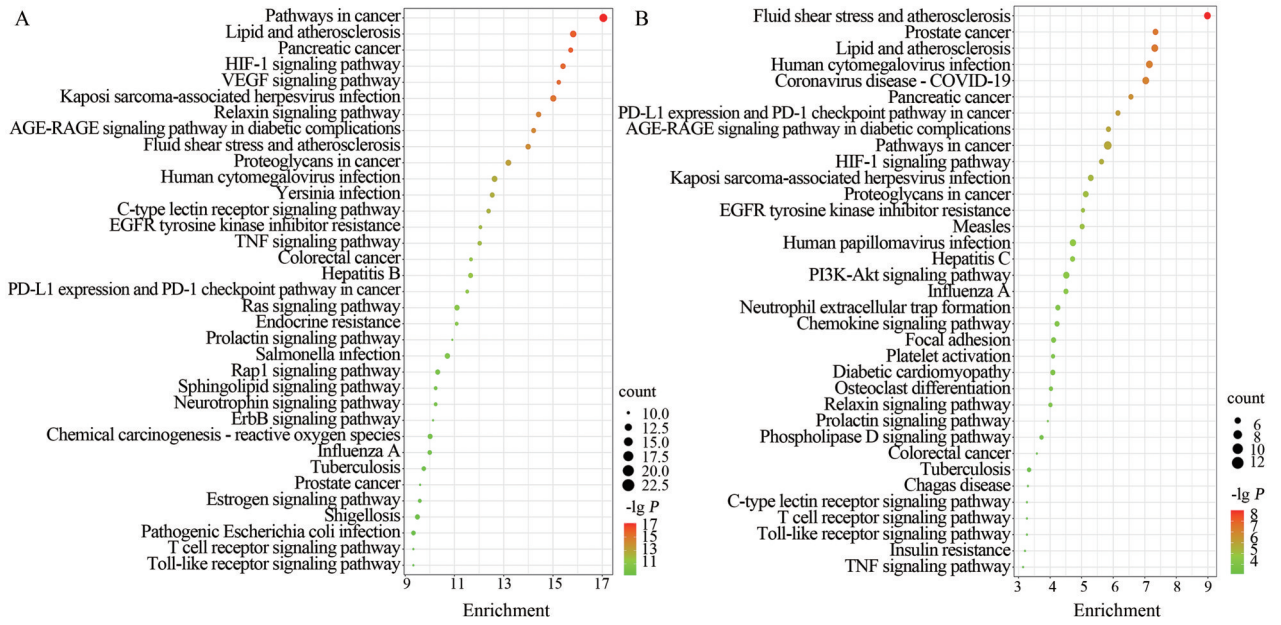


**Figure 6** KEGG enrichment analysis of influenza-related target proteins (A) and COVID-19-related target proteins (B). KEGG: Kyoto encyclopedia of genes and genomes

**Table 2** Molecular docking results for components and targets of Isatidis Radix in the prevention of influenza

| Target | PDB ID | Compound | Polar bonding | Binding energy /kcal·mol$^{-1}$ |
|---|---|---|---|---|
| AKT1 | 4GV1 | 0XZ(Capivasertib) | ALA230, GLU234, GLU278, GLU228 | – |
| | | Tryptanthrin | ALA230, GLU228, THR211 | −7.25 |
| | | Isaindigodione | THR160, PHE161, LYS158 | −6.22 |
| | | Indole-3-acetonitrile-6-*O*-*β*-*D*-glucopyranoside | GLU234, LYS158, ASP292 | −6.20 |
| | | 1-Methoxyindole-3-acetamide | ALA230, GLU234, THR291 | −6.07 |
| | | 2,3-Dihydro-1*H*-pyrrolo[2,1-*c*][1,4]benzodiazepine-5,11(10*H*,11a*H*)-dione | ALA230, GLU228 | −5.98 |
| ALB | 7QFE | 4TX(Gemfibrozil) | SER489, TYR411 | – |
| | | Tryptanthrin | LYS414, PHE488 | −8.48 |
| | | Isaindigodione | TYR411, LYS414, ARG410 | −9.2 |
| | | Indole-3-acetonitrile-6-*O*-*β*-*D*-glucopyranoside | TYR411 | −6.89 |
| | | 1-Methoxyindole-3-acetamide | LYS414 | −6.69 |
| | | 2,3-Dihydro-1*H*-pyrrolo[2,1-*c*][1,4]benzodiazepine-5,11(10*H*,11a*H*)-dione | – | −7.47 |
| GAPDH | 6M61 | F4F | THR211, GLY212, CYS152 | – |
| | | Tryptanthrin | ALA183, ASN316 | −7.63 |
| | | Isaindigodione | CYS152, ARG234, THR182, THR184 | −6.91 |
| | | Indole-3-acetonitrile-6-*O*-*β*-*D*-glucopyranoside | THR211, ALA150, ASN316, ARG234 | −5.18 |
| | | 1-Methoxyindole-3-acetamide | CYS152, ALA150, ASN316, SER122 | −5.96 |
| | | 2,3-Dihydro-1*H*-pyrrolo[2,1-*c*][1,4]benzodiazepine-5,11(10*H*,11a*H*)-dione | ASN316 | −5.88 |
| VEGFA | 1MKK | Tryptanthrin | CYS60 | −7.16 |
| | | Isaindigodione | CYS60, CYS26, SER50 | −7.22 |
| | | Indole-3-acetonitrile-6-*O*-*β*-*D*-glucopyranoside | SER50, PHE47, TYR45, ASP34, ILE35, PHE36 | −6.3 |
| | | 1-Methoxyindole-3-acetamide | CYS60, CYS26, SER50 | −5.99 |
| | | 2,3-Dihydro-1*H*-pyrrolo[2,1-*c*][1,4]benzodiazepine-5,11(10*H*,11a*H*)-dione | CYS60 | −6.73 |
| SRC | 2QXW | LDT(IDD 594) | TYR48, HIS110, TRP111 | – |
| | | Tryptanthrin | TYR309 | −9.01 |
| | | Isaindigodione | – | −9.35 |
| | | Indole-3-acetonitrile-6-*O*-*β*-*D*-glucopyranoside | TRP111, THR113 | −8.06 |
| | | 1-Methoxyindole-3-acetamide | TRP111 | −7.46 |
| | | 2,3-Dihydro-1*H*-pyrrolo[2,1-*c*][1,4]benzodiazepine-5,11(10*H*,11a*H*)-dione | – | −8.61 |

**Table 3** Molecular docking results for components and targets of Isatidis Radix in the prevention of COVID-19.

| Target | PDB ID | Compound | Polar bonding | Binding energy /kcal·mol$^{-1}$ |
|---|---|---|---|---|
| ALB | 7QFE | 4TX(Gemfibrozil) | SER489, TYR411 | − |
| | | Tryptanthrin | LYS414, PHE488 | −8.48 |
| | | Deoxyvasicinone | PHE488, LYS414 | −6.86 |
| | | 2,3-Dihydro-1*H*-pyrrolo[2,1-*c*][1,4]benzodiazepine-5,11(10*H*,11a*H*)-dione | − | −7.47 |
| | | 1-Methoxyindole-3-acetamide | LYS414 | −6.69 |
| | | 1-Methoxyindole-3-carboxaldehyde | PHE488, LYS414 | −5.72 |
| AKT1 | 4GV1 | 0XZ(Capivasertib) | ALA230, GLU234, GLU278, GLU228 | − |
| | | Tryptanthrin | ALA230, GLU228, THR211 | −7.25 |
| | | Deoxyvasicinone | ALA230 | −5.61 |
| | | 2,3-Dihydro-1*H*-pyrrolo[2,1-*c*][1,4]benzodiazepine-5,11(10*H*,11a*H*)-dione | ALA230, GLU228 | −5.98 |
| | | 1-Methoxyindole-3-acetamide | ALA230, GLU234, THR291 | −6.07 |
| | | 1-Methoxyindole-3-carboxaldehyde | ALA230 | −4.99 |
| VEGFA | 1MKK | Tryptanthrin | CYS60 | −7.16 |
| | | Deoxyvasicinone | CYS60, SER24 | −6.27 |
| | | 2,3-Dihydro-1*H*-pyrrolo[2,1-*c*][1,4]benzodiazepine-5,11(10*H*,11a*H*)-dione | CYS60 | −6.73 |
| | | 1-Methoxyindole-3-acetamide | CYS60, CYS26, SER50 | −5.99 |
| | | 1-Methoxyindole-3-carboxaldehyde | SER50 | −5.22 |
| EGFR | 6J6M | BA0 | GLU475, MET477, THR474 | − |
| | | Tryptanthrin | MET477, THR474, LYS430 | −6.9 |
| | | Deoxyvasicinone | SER538 | −6.17 |
| | | 2,3-Dihydro-1*H*-pyrrolo[2,1-*c*][1,4]benzodiazepine-5,11(10*H*,11a*H*)-dione | THR474 | −6.81 |
| | | 1-Methoxyindole-3-acetamide | GLU475, MET477, THR474, LYS430 | −6.27 |
| | | 1-Methoxyindole-3-carboxaldehyde | THR474, LYS430 | −5.06 |
| ICAM1 | 3BQN | BQN | LYS305, TYR166 | − |
| | | Tryptanthrin | LYS305 | −7.31 |
| | | Deoxyvasicinone | − | −5.83 |
| | | 2,3-Dihydro-1*H*-pyrrolo[2,1-*c*][1,4]benzodiazepine-5,11(10*H*,11a*H*)-dione | − | −6.27 |
| | | 1-Methoxyindole-3-acetamide | GLU284, LYS305 | −5.94 |
| | | 1-Methoxyindole-3-carboxaldehyde | LYS305 | −5.49 |

“成分−靶点−通路”整体入手, 探讨板蓝根防治流感和COVID-19的作用机制。

本文将33个入血成分和文献支持的8个有效成分作为活性成分, 采用网络药理学预测到板蓝根防治流感的AKT1、ALB、GAPDH、VEGFA、SRC等39个核心靶点; 防治COVID-19的ALB、AKT1、VEGFA、EGFR、ICAM1等34个核心靶点。AKT1、SRC、EGFR在细胞信号传导中具有关键作用, 靶向治疗能够增强细胞抗病毒宿主防御[33,34]; GAPDH是细胞调节因子, 参与DNA修复以及细胞凋亡等生物过程[35]; ALB是维持血液渗透压的重要物质, VEGF调节血管重塑, 两者均对炎症反应有调节作用[36,37]。ALB、VEGFA、ICAM1等蛋白是感染COVID-19的潜在诊断以及预后生物标志物, 其中ICAM1促进白细胞、T细胞迁移至炎症部位, 对免疫反应具有重要作用[38-40]。由此可推测出板蓝根防治流感主要作用靶点与细胞信号传导、细胞凋亡、炎症反应等密切相关; 防治COVID-19主要作用靶点与细胞信号传导、细胞黏附、迁移、免疫反应等密切相关。

通路富集结果显示, 板蓝根防治流感和COVID-19通过HIF-1、VEGF、TNF、甲型流感、TLR、PI3K-AKT和COVID-19等信号通路。HIF-1、TNF、PI3K-AKT均是参与信号传导、炎症反应、免疫调节的重要通路[41,42], VEGF信号通路诱导内皮细胞增殖、促进细胞迁移、抑制细胞凋亡, 与流感以及COVID-19病毒感染密切相关[43-45]。TNF信号通路与HIF-1信号通路有很强的关联, HIF-1$\alpha$会促进新冠病毒的感染并加重炎症反应; 病毒通过PI3K-AKT通路影响各种细胞功能, 细胞防御机制激活后, 高活性PI3K-AKT通路可能会阻碍病毒传播[46]。有研究表明, TLR-EGFR信号通路参与病毒感染后的气道重塑[47,48]。以上结果在相关文献[22,24,49]中有相似报道, 对板蓝根防治流感和COVID-19的作用机制提供佐证。虽然本研究发现板蓝根防治流感和COVID-19的作用机制相似, 根据假定值$P$推测板蓝根防治流感主要通过HIF-1、VEGF、TNF等信号通路调节炎症与免疫反应; 板蓝根防治COVID-19主要通过COVID-19、HIF-1、PI3K-AKT等信号通路参与调节和防御机制。

根据分子对接结果可知, 色胺酮、依靛蓝酮、吲哚-

3-乙腈-6-*O*-*β*-*D*-吡喃葡萄糖苷、1-甲氧基-吲哚-3-乙酰胺、[2,3-二氢-1*H*-吡咯并[2,1-*c*][1,4]苯并二氮杂䓬-5,11(10*H*,11a*H*)-二酮] 等成分可能作用于AKT1、ALB、GAPDH、VEGFA、SRC等靶点防治流感; 色胺酮、脱氧鸭嘴花碱酮、[2,3-二氢-1*H*-吡咯并[2,1-*c*][1,4]苯并二氮杂䓬-5,11(10*H*,11a*H*)-二酮]、1-甲氧基吲哚-3-乙酰胺、1-甲氧基吲哚-3-甲醛等成分可能作用于ALB、AKT1、VEGFA、EGFR、ICAM1等靶点防治COVID-19。依靛蓝酮对神经氨酸酶有抑制活性, 起到抗病毒的作用[50]; 色胺酮对甲型流感病毒和新型冠状病毒表现出潜在的抑制活性, 具有抗炎和抗病毒的潜力[51-53]; 有研究表明, 吲哚-3-乙腈-6-*O*-*β*-*D*-吡喃葡萄糖苷具有抗多种甲型流感病毒活性, 可显著抑制流感病毒引起的小鼠肺组织病变[54,55]。脱氧鸭嘴花碱酮具有一定的抗菌抗炎活性[56]。“核心成分−关键靶点”分子对接结果均具有较小的结合能, 且部分成分与靶点结合位点和阳性药与靶点结合位点基本吻合, 说明板蓝根核心成分与疾病相关靶点有较好的结合活性。已有文献[22,49]通过网络药理学筛选出板蓝根防治流感和COVID-19的核心成分为生物碱、黄酮、木脂素类化合物, 本研究主要筛选出生物碱与核苷类化合物, 为板蓝根的药效物质选择提供了依据。

综上所述, 板蓝根防治流感和COVID-19是通过多成分、多靶点、多途径协同发挥作用机制, 这对后续药物开发及临床应用具有参考意义。

**作者贡献**: 王星琪负责本文的选题与设计、方法建立、实验数据处理、撰写文章等; 常金在前期方法摸索及数据处理方面提供了帮助; 张倩对实验思路、文章修改提供了指导; 林丽娜在样品制备及数据处理方面提供了帮助; 邵平提供了本文的相关实验材料; 李清在选题与设计、实验思路、方法建立及文章修改提供了宝贵意见。

**利益冲突**: 无任何利益冲突。

## References

[1] Shi X, Zhang HY, Miao Q, et al. Scoping review of treatment of influenza with oral proprietary Chinese medicines [J]. Chin J Exp Tradit Med Form (中国实验方剂学杂志), 2022. https://kns.cnki.net/kcms/detail/11.3495.R.20220227.0923.001.html.

[2] Li P, Hu S, Qian C, et al. The therapeutic effect of traditional Chinese medicine on inflammatory diseases caused by virus, especially on those caused by COVID-19 [J]. Front Pharmacol, 2021, 12: 650425.

[3] Huang K, Zhang P, Zhang ZH, et al. Traditional Chinese medicine (TCM) in the treatment of COVID-19 and other viral infections: efficacies and mechanisms [J]. Pharmacol Ther, 2021, 225: 107843.

[4] Yang L, Wang HQ, Li YH. Research progress on therapeutic drugs for corona virus disease 2019 [J]. Acta Pharm Sin (药学学报), 2020, 55: 1081-1090.

[5] Wang HR, Wang Q. Advances in research of novel coronavirus related drugs and biological products [J]. Acta Pharm Sin (药学学报), 2020, 55: 349-354.

[6] Chinese Pharmacopoeia Commission. Pharmacopoeia of the People's Republic of China (中华人民共和国药典) [S]. 2020 Ed. Part I. Beijing: China Medical Science Press, 2020: 214-215.

[7] Deng JL, Tao YL, He YQ, et al. Research progress on active components and mechanism of Isatidis Radix for influenza virus [J]. Chin J Chin Mater Med (中国中药杂志), 2021, 46: 2029-2036.

[8] Chen J, Zhu ZP, Gao TH, et al. Isatidis Radix and Isatidis Folium: a systematic review on ethnopharmacology, phytochemistry and pharmacology [J]. J Ethnopharmacol, 2022, 283: 114648.

[9] Ma X, Wei RN, Zhao LH. Study on the clinical application and dose-effect relationship of isatis root [J]. J Changchun Univ Tradit Chin Med (长春中医药大学学报), 2022, 38: 145-148.

[10] Yang KL, Gao Y, Yang FW, et al. Analysis of traditional Chinese medicine from patent information sharing platform of coronavirus disease 2019 (COVID-19) [J]. Chin J Chin Mater Med (中国中药杂志), 2020, 45: 3001-3006.

[11] Jung EH, Jung JY, Ko HL, et al. Tryptanthrin prevents oxidative stress-mediated apoptosis through AMP-activated protein kinase-dependent p38 mitogen-activated protein kinase activation [J]. Arch Pharm Res, 2017, 40: 1071-1086.

[12] Jie C, Luo Z, Chen H, et al. Indirubin, a bisindole alkaloid from Isatis indigotica, reduces H1N1 susceptibility in stressed mice by regulating MAVS signaling [J]. Oncotarget, 2017, 8: 105615-105629.

[13] Tu P, Tian R, Lu Y, et al. Beneficial effect of Indigo Naturalis on acute lung injury induced by influenza A virus [J]. Chin Med, 2020, 15: 128.

[14] Chang SJ, Chang YC, Lu KZ, et al. Antiviral activity of isatis indigotica extract and its derived indirubin against Japanese encephalitis virus [J]. Evid Based Complement Alternat Med, 2012, 2012: 925830.

[15] Xiao P, Ye WY, Chen JW, et al. Antiviral activities against influenza virus (FM1) of bioactive fractions and representative compounds extracted from Banlangen (Radix Isatidis) [J]. J Tradit Chin Med, 2016, 36: 369-376.

[16] Zeng JX, Zhou W, Jiang YT, et al. Antiviral and anti-inflammatory mechanism of anti-601 mixture based on network pharmacology and molecular docking [J]. J China Pharm Univ (中国药科大学学报), 2020, 51: 577-583.

[17] Zhang YR, Gan ZQ, Liu ZX, et al. Exploring mechanism of Qingkailing Injection in treatment of coronavirus disease 2019 (COVID-19) based on network pharmacology and molecular docking [J]. Chin Tradit Herbal Drugs (中草药), 2020, 51: 3201-

3210.

[18] Yao YX, He ZX, Liu XF, et al. Potential material basis of Kangbingdu Granules for treatment of coronavirus disease 2019 (COVID-19) based on network pharmacology and molecular docking technology [J]. Chin Tradit Herb Drugs (中草药), 2020, 51: 1386-1396.

[19] Yang AX, Lu L, Liu YW. Mechanism of antipyretic and anti-inflammation actions of Tuire Jieduling based upon network pharmacology and molecular docking methods [J]. Chin J Hosp Pharm (中国医院药学杂志), 2021, 41: 2186-2191.

[20] Cao C, Cui Y, Chu YX, et al. Investigation on mechanism and active components of Shufeng Jiedu Capsule in treatment of COVID-19 based on network pharmacology and molecular docking [J]. Chin Tradit Herbal Drugs (中草药), 2020, 51: 2283-2296.

[21] Yan HY, Zou CC. Mechanism and material basis of Lianhua Qingwen capsule for improving clinical cure rate of COVID-19: a study based on network pharmacology and molecular docking technology [J]. J South Med Univ (南方医科大学学报), 2021, 41: 20-30.

[22] Deng JL, Ma Y, He YQ, et al. A network pharmacology-based investigation to the pharmacodynamic material basis and mechanisms of the anti-inflammatory and anti-viral effect of isatis indigotica [J]. Drug Des Devel Ther, 2021, 15: 3193-3206.

[23] Xu JL, Jiang W, Pang XC, et al. Network pharmacology study of the effective constituents in the Compound Yizhihao against influenza disease [J]. Acta Pharm Sin (药学学报), 2017, 52: 745-752.

[24] Yu B, Lin F, Ning H, et al. Network pharmacology study on the mechanism of the Chinese medicine Radix Isatidis (Banlangen) for COVID-19 [J]. Medicine, 2021, 100: e26881.

[25] Niu M, Zhang SQ, Zhang B, et al. Interpretation of network pharmacology evaluation method guidance [J]. Chin Tradit Herb Drugs (中草药), 2021, 52: 4119-4129.

[26] Sampei M, Arai MA, Ishibashi M. Total syntheses of schizandriside, saracoside and (+/−)-isolariciresinol with antioxidant activities [J]. J Nat Med, 2018, 72: 651-654.

[27] Xiao P, Li X, Chen JW, et al. Simultaneous quantification of three chemical types bioactive compounds in Radix Isatidis and its relevant pharmaceutical dosage forms by HPLC-DAD [J]. J Braz Chem Soc, 2017, 28: 1237-1246.

[28] Yu J, Zhang YH, Ning SJ, et al. Molecular cloning and metabolomic characterization of the 5-enolpyruvylshikimate-3-phosphate synthase gene from *Baphicacanthus cusia* [J]. BMC Plant Biol, 2019, 19: 485.

[29] Sun Q, Leng J, Tang L, et al. A comprehensive review of the chemistry, pharmacokinetics, pharmacology, clinical applications, adverse events, and quality control of Indigo Naturalis [J]. Front Pharmacol, 2021, 12: 664022.

[30] Ye WY, Li X, Cheng JW. Screening of eleven chemical constituents from Radix isatidis for antiviral activity [J]. Afr J Pharm Pharmacol, 2011, 5: 1932-1936.

[31] Ma Z, Guan M, Xing ZF, et al. Research status and progress of influenza viruse [J]. Lab Med (检验医学), 2020, 35: 1315-1319.

[32] Huang C, Wang Y, Li X, et al. Clinical features of patients infected with 2019 novel coronavirus in Wuhan, China [J]. Lancet, 2020, 395: 497-506.

[33] Casalino-Matsuda SM, Chen F, Gonzalez-Gonzalez FJ, et al. Hypercapnia suppresses macrophage antiviral activity and increases mortality of influenza A infection *via* Akt1 [J]. J Immunol, 2020, 205: 489-501.

[34] Zheng K, Kitazato K, Wang YF. Viruses exploit the function of epidermal growth factor receptor [J]. Rev Med Virol, 2014, 24: 274-286.

[35] Rizvi SHM, Shao D, Tsukahara Y, et al. Oxidized GAPDH transfers *S*-glutathionylation to a nuclear protein sirtuin-1 leading to apoptosis [J]. Free Radic Biol Med, 2021, 174: 73-83.

[36] Deng Y, Li Q, Li M, et al. Network pharmacology identifies the mechanisms of Sang-Xing-Zhi-Ke-Fang against pharyngitis [J]. Evid Based Complement Alternat Med, 2020, 2020: 2421916.

[37] Lee CG, Link H, Baluk P, et al. Vascular endothelial growth factor (VEGF) induces remodeling and enhances TH2-mediated sensitization and inflammation in the lung [J]. Nat Med, 2004, 10: 1095-1103.

[38] Kaur S, Hussain S, Kolhe K, et al. Elevated plasma ICAM1 levels predict 28-day mortality in cirrhotic patients with COVID-19 or bacterial sepsis [J]. JHEP Rep, 2021, 3: 100303.

[39] Liu GL, Zhang BC, Zhang SW, et al. LDH, CRP and ALB predict nucleic acid turn negative within 14 days in symptomatic patients with COVID-19 [J]. Scott Med J, 2021, 66: 108-114.

[40] Mao SY, Liu CJ, Xu F. Research progress of sICAM-1 as a infection marker [J]. J Mod Med Healt (现代医药卫生), 2014, 30: 1192-1194.

[41] He YC, Zhang J, Feng JJ, et al. The role of hypoxia inducible factor-1$\alpha$ on inflammation mediated by H1N1 infected macrophage [J], J Microbes Infect (微生物与感染), 2021, 16: 164-170.

[42] Zhou J, Callapina M, Goodall GJ, et al. Functional integrity of nuclear factor kappa B, phosphatidylinositol 3'-kinase, and mitogen-activated protein kinase signaling allows tumor necrosis factor alpha-evoked Bcl-2 expression to provoke internal ribosome entry site-dependent translation of hypoxia-inducible factor 1 alpha [J]. Cancer Res, 2004, 64: 9041-9048.

[43] Yin YD, Cao D, Shen H, et al. Differential circRNA expression profiles in peripheral blood mononuclear cells among mild and severe influenza-associated pneumonia patients [J]. Natl Med J China (中华医学杂志), 2021, 101: 573-578.

[44] Tian MF, Liu WY, Li X, et al. HIF-1 alpha promotes SARS-CoV-2 infection and aggravates inflammatory responses to COVID-19 [J]. Signal Transduct Target Ther, 2021, 6: 308.

[45] Yang ZH, Zou XG, Feng PQ, et al. Inhibition of the PI3K/AKT signaling pathway or overexpression of beclin1 blocks reinfec-

tion of streptococcus pneumoniae after infection of influenza A virus in severe community-acquired pneumonia [J]. Inflammation, 2019, 42: 1741-1753.

[46] Ji WT, Liu JH. PI3K-Akt signaling and viral infection [J]. Recent Pat Biotechnol, 2008, 2: 218-226.

[47] Jiang JJ, Wang YH, Tang XP, et al. Regulation of viral infection-induced airway remodeling cytokine production by the TLR3-EGFR signaling pathway in human bronchial epithelial cells [J]. COPD, 2016, 13: 750-755.

[48] Merkle M, Ribeiro A, Sauter M, et al. Effect of activation of viral receptors on the gelatinases MMP-2 and MMP-9 in human mesothelial cells [J]. Matrix Biol, 2010, 29: 202-208.

[49] Liu MC, Yang L, Hu YH. Research on the potential mechanism of Banlangen in the treatment of COVID-19 *via* network pharmacology and molecular docking [J]. Pharm Clin Chin Mater Med (中药与临床), 2022, 13: 51-57, 99.

[50] Hou XB. Research of the Potential Pharmacodynamic Ingredients of Radix Isatidis and Its Mechanism (板蓝根潜在药效成分的发现及其作用机制的研究) [D]. Nanjing: Nanjing University of Chinese Medicine, 2017.

[51] Cai CP, Xu L, Fang JF, et al. *In silico* prediction and bioactivity evaluation of chemical ingredients against influenza A virus from *Isatis tinctoria* L. [J]. Front Pharmacol, 2021, 12: 755396.

[52] Zhang XY, Xia J, Zhang WJ, et al. Study on pharmacokinetics and tissue distribution of single dose oral tryptanthrin in Kunming mice by validated reversed-phase high-performance liquid chromatography with ultraviolet detection [J]. Integr Med Res, 2017, 6: 269-279.

[53] Harwansh RK, Bahadur S. Herbal medicines to fight against COVID-19: new battle with an old weapon [J]. Curr Pharm Biotechnol, 2022, 23: 244-269.

[54] Dong JH, Yan FM, Li S, et al. Multigram scale synthesis and anti-Influenza activity of 3-indoleacetonitrile glucosides [J]. Nat Prod Commun, 2020, 15: 1-9.

[55] Zhu Q, Yang ZF, Li CY, et al. Application of indole-3-acetonitrile-6-*O*-beta-*D*-pyran glucoside in pharmacy: CN, 102836168B [P]. 2014-06-18 [2022-04-08].

[56] Khodarahmi G, Jafari E, Hakimelahi G, et al. Synthesis of some new quinazolinone derivatives and evaluation of their antimicrobial activities [J]. Iran J Pharm Res, 2012, 11: 789-797.